Signature of the s-Wave Regime High above Ultralow Temperatures

Robin Côté and Ionel Simbotin
Department of Physics, U-3046, University of Connecticut, 2152 Hillside Road, U-3046 Storrs, Connecticut 06269-3046, USA

(Received 15 June 2018; published 25 October 2018)

Resonant exchange is a general process playing a key role in many-body dynamics and transport phenomena, such as spin, charge, or excitation diffusion. The underlying process is described by the resonant exchange cross section. We show that the s-wave scattering, generally thought to contribute mainly in the ultracold (or Wigner) regime, dictates the overall cross section over a broad range of energies. We derive an analytical expression and explain its applicability high above the Wigner regime. In particular, we demonstrate its relationship to the classical capture (Langevin) cross section and apply it to three very different resonant processes: namely, resonant charge transfer, spin flip, and excitation exchange. This expression explains large variations for different isotopes that cannot otherwise be accounted for by the small change in mass. The s-wave signature also allows us to gain information about the Wigner regime from data obtained at much higher temperatures, which is especially advantageous for systems where the ultracold regime is not reachable.

DOI: 10.1103/PhysRevLett.121.173401

The quantal regime, in which the quantum nature of phenomena plays a pivotal role, is at the forefront of research in many areas of physics. This is particularly well illustrated by various achievements at ultracold temperatures, which range from the control of few-body interactions, e.g., using tunable Feshbach resonances [1,2] to explore degenerate quantum gases [3,4] or exotic three-body Efimov states [5,6], to control of internal and motional states to explore many-body dynamics [7], including studies of new phases or quantum simulations [8,9]. In recent years, rapid progress has been made to extend the types of systems investigated from atomic to molecular [10–13] and ionic species [14,15]. However, for many of them, e.g., atom-ion hybrid systems [16–24], the quantum regime dominated by s-wave scattering is still outside the reach of today's experimental techniques.

In many ultracold studies, resonant exchange plays a central role, e.g., in Rydberg samples [25] where excitation exchange is involved in Föster resonances [25,26] or quantum random walk [27]. Other examples relate to spin exchange, e.g., between ultracold atoms and molecules [28–31] or in two-orbital interactions with SU(N) symmetry [32]. Recently, atom-exchange reactions between NaK Feshbach molecules and K atoms were investigated as an effective spin-exchange interaction [33]. Resonant exchange between two asymptotically degenerate states can be understood as the interference of two interaction paths and has been studied in the scattering of neutral atoms, e.g., spin flip in alkali atom collisions [34,35] with singlet and triplet potential curves, as well as in S-P excitation exchange for identical atoms [36], and charge transfer between an ion and its neutral parent atom [37,38]. Recent experiments with atom-ion systems have observed spin-flip dynamics above the Wigner regime in $Yb^+ + {}^{87}Rb$ [20], $Yb^+ + {}^{6}Li$ [39], and $^{88}Sr^+ + Rb$ [40,41]. For such systems, reaching the Wigner regime is difficult, and probing s-wave scattering at higher temperatures will provide essential information. In cases involving quasiresonant scattering, e.g., in isotope exchange, the resonant approximation adequately describes the system if the scattering energy is higher than the energy splitting between the asymptotic states [42,43].

In this Letter, we study the resonant exchange process

$$X^{\alpha} + X^{\alpha'} \rightarrow X^{\alpha'} + X^{\alpha}, \tag{1}$$

where α and α' denote internal states, such as charges 0 and +1 in charge transfer $X + X^+ \rightarrow X^+ + X$, or electronic states S and P in excitation exchange $X(S) + X(P) \rightarrow X(P) + X(S)$. The corresponding cross section reads [14,37,44]

$$\sigma_{\rm exc}(E) = \frac{\pi}{k^2}\sum_{\ell=0}^{\infty}(2\ell+1)\sin^2(\eta_\ell^a - \eta_\ell^b), \tag{2}$$

where $k = \sqrt{2\mu E/\hbar^2}$, with reduced mass μ and collision energy E. Here, $\eta_\ell^{a/b}$ is the ℓth partial wave scattering phase shift along the potential $V_{a/b}$ corresponding to the asymptotically degenerate channels a/b (e.g., singlet or triplet states). We consider inverse power-law tails $V \sim -C_n/r^n$ with $n > 2$.

For energies high above the Wigner regime, many partial waves contribute; we thus regard ℓ as a continuous variable and use a semiclassical expression based on the Wentzel-Kramers-Brillouin (WKB) approximation [44,45]

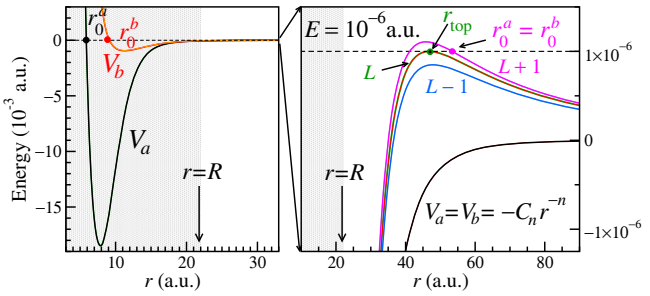

FIG. 1. Typical $V_{a/b}$ (black/red) and turning points $r_0^{a/b}$ ($r \le R$ is shaded). Right panel: $V_a = V_b = -(C_n/r^n)$ for $r > R$ leading to identical centrifugal barriers. For $\ell = L$, the barrier reaches the scattering energy $E = 10^{-6}$ a.u. (~300 mK); as ℓ grows, the turning points move "suddenly" from the short-range shaded region ($L-1$) to the top (L) and outer side of the barrier ($L+1$). Here, a/b stands for the singlet or triplet state of Rb_2 with $L \approx 22.4$.

$$\frac{\partial \eta_\ell^i}{\partial \ell} \approx \frac{\pi}{2} + \int_{r_0^i(\ell)}^{\infty} dr \frac{\partial}{\partial \ell}\left(\frac{2\mu}{\hbar^2}[E - V_i(r)] - \frac{(\ell+\frac{1}{2})^2}{r^2}\right)^{1/2}, \tag{3}$$

where $r_0^i(\ell)$ is the classical turning point. Defining $F_{i,\ell}(r) \equiv [(2\mu/\hbar^2)[E - V_i(r)] - (\ell+\frac{1}{2})^2/r^2]^{-1/2}$, we write

$$\frac{\partial \eta_\ell^i}{\partial \ell} \approx \frac{\pi}{2} - \left(\ell+\frac{1}{2}\right)\int_{r_0^i(\ell)}^{\infty} \frac{dr}{r^2} F_{i,\ell}(r) \equiv \frac{\pi}{2} - \left(\ell+\frac{1}{2}\right) A_i(\ell). \tag{4}$$

Although ℓ can be large, we assume that the centrifugal term $(\ell+\frac{1}{2})^2/r^2$ is small enough that the wave function still probes the inner region, i.e., $\ell < L$ with L defined by $\hbar^2(L+\frac{1}{2})^2/r_{top}^2 \equiv 2\mu[E - V(r_{top})]$. As shown in Fig. 1, when the top of the centrifugal barrier located at r_{top} is below E, $r_0^i(\ell)$ is deep inside the short-range region, moving suddenly to r_{top} at L and to the outer region for $\ell > L$. The centrifugal barrier appears at values of r where the potential is given by its asymptotic form $V(r) \simeq -C_n/r^n$, allowing us to split $A_i(\ell)$ into two regions, below and above R, with $R < r_{top}$,

$$\begin{aligned} A_i(\ell) &= \int_{r_0^i(\ell)}^{R} \frac{dr}{r^2} F_{i,\ell}(r) \\ &\quad + \int_R^{\infty} \frac{dr}{r^2}\left[\frac{2\mu}{\hbar^2}\left(E + \frac{C_n}{r^n}\right) - \frac{(\ell+\frac{1}{2})^2}{r^2}\right]^{-\frac{1}{2}} \\ &\equiv A_i(\ell, R) + A_i^{\infty}(\ell, R). \end{aligned} \tag{5}$$

We are interested in $\Delta\eta_\ell \equiv \eta_\ell^a - \eta_\ell^b$ in Eq. (2) and noting that $A_a^{\infty}(\ell, R) = A_b^{\infty}(\ell, R)$, we use Eq. (4) to obtain

$$\begin{aligned} \frac{\partial \Delta\eta_\ell}{\partial \ell} &= -\left(\ell+\frac{1}{2}\right)[A_a(\ell, R) - A_b(\ell, R)] \\ &\equiv -\left(\ell+\frac{1}{2}\right)\Delta A(\ell). \end{aligned} \tag{6}$$

At short range ($r \le R$), $\hbar^2(\ell+\frac{1}{2})^2/r^2 \ll 2\mu[E - V(r)]$, and we can expand $F_{i,\ell} \approx F_{i,\ell=0} + \mathcal{O}(\ell^2)$, so that to leading order, $A_i(\ell, R) \approx \int_{r_0^i(\ell)}^{R}(dr/r^2)F_{i,\ell=0}(r)$. We can then neglect the ℓ dependence of $r_0(\ell)$ (see Fig. 1) and take its s-wave value $r_0(\ell) \equiv r_0$ so that $\Delta A(\ell) \approx \Delta A_0$ is then ℓ independent, and Eq. (6) becomes $\partial(\eta_\ell^a - \eta_\ell^b)/\partial\ell \approx -(\ell+\frac{1}{2})\Delta A_0$. Integrating over ℓ leads to $\Delta\eta_\ell \approx (\eta_0^a - \eta_0^b) - \ell(\ell+1)\Delta A_0$. Using the Levinson theorem [44,45] to write $\eta_0^{a/b} = N^{a/b}\pi + \delta_0^{a/b}$, where $\delta_0^{a/b}$ is the s-wave phase shift modulo π, and $N^{a/b}$ is the number of bound states supported by $V_{a/b}$, we finally have

$$\Delta\eta_\ell \approx \pi\Delta N + \Delta\delta_0 - \ell(\ell+1)\Delta A_0, \tag{7}$$

where $\Delta N = N_a - N_b$, $\Delta\delta_0 = \delta_0^a - \delta_0^b$, and

$$\Delta A_0 = \int_{r_0^a(E)}^{R} \frac{dr}{r^2} F_{a,\ell=0}(r) - \int_{r_0^b(E)}^{R} \frac{dr}{r^2} F_{b,\ell=0}(r). \tag{8}$$

The inner turning point r_0^i depends slightly on the scattering energy E, and typically, ΔA_0 varies little with E, and is of the order 0.01–0.001 for the physical systems considered in this Letter, with ΔA_0 smaller for heavier systems due the 2μ factor.

Returning to the cross section, we approximate the sum in Eq. (2) with an integral $\sigma_{exc} \approx (\pi/k^2)\int_0^{\infty} d\ell(2\ell+1)\sin^2(\eta_\ell^a - \eta_\ell^b)$ and write using Eq. (7)

$$\sigma_{exc} \approx \frac{\pi}{k^2}\int_0^{L} d\ell(2\ell+1)\sin^2\left(\Delta\delta_0 - \ell(\ell+1)\frac{\Delta A_0}{2}\right). \tag{9}$$

The upper limit is set to L since the phase shift difference is negligible for $\ell \ge L$, as discussed above [37]. Defining $x \equiv \Delta\delta_0 - \frac{1}{2}\ell(\ell+1)\Delta A_0$, our integral simply becomes $\sigma_{exc} \simeq -(\pi/k^2)(2/\Delta A_0)\int_{x_0}^{x_L} dx\sin^2 x = -(\pi/k^2)(2/\Delta A_0)[(x/2) - \frac{1}{4}\sin(2x)]_{x_0}^{x_L}$, with $x_0 = \Delta\delta_0$ and $x_L = \Delta\delta_0 - \frac{1}{2}L(L+1)\Delta A_0$, giving

$$\begin{aligned} \sigma_{exc} \simeq \frac{\pi}{k^2}\frac{1}{\Delta A_0}\Bigg(&L(L+1)\frac{\Delta A_0}{2} - \frac{1}{2}\sin(2\Delta\delta_0) \\ &+ \frac{1}{2}\sin(2\Delta\delta_0 - L(L+1)\Delta A_0)\Bigg). \end{aligned} \tag{10}$$

With $L(L+1)\Delta A_0$ small, we find $\sin[2\Delta\delta_0 - L(L+1)\Delta A_0] \approx \sin(2\Delta\delta_0) - L(L+1)\Delta A_0\cos(2\Delta\delta_0)$ and with $L(L+1) \approx L^2$,

TABLE I. Langevin cross section σ_L for various n.

n	3	4	6
σ_L	$3\pi(C_3/2E)^{2/3}$	$2\pi(C_4/E)^{1/2}$	$(3\pi/2)(2C_6/E)^{1/3}$

$$\sigma_{\rm exc}(E) \simeq \frac{\pi}{k^2}\frac{1}{\Delta A_0}L(L+1)\frac{\Delta A_0}{2}[1-\cos(2\Delta\delta_0)] \approx \frac{\pi}{k^2}L^2\sin^2\Delta\delta_0(E), \tag{11}$$

which is related to the Langevin cross section σ_L defined by the maximum impact parameter $b_{\rm max}$ still allowing colliding partners to reach the short-range region where the exchange process occurs with unit probability [14,37,44]. With $b \equiv (\ell+\frac{1}{2})/k$, $b_{\rm max}$ is obtained for $\ell = L$, as the centrifugal barrier prevents access into short range for $\ell > L$ (see Fig. 1). Thus,

$$\sigma_L(E) = \pi b_{\rm max}^2 \simeq \frac{\pi}{k^2}L^2, \tag{12}$$

where $L+\frac{1}{2} \approx L$, and $L(E)$ is obtained from $E = V(r_{\rm top})$. The top of the barrier for $V(r) \sim -C_n/r^n$ asymptotic potentials is located at $r_{\rm top} = \{[\mu n C_n]/[\ell(\ell+1)\hbar^2]\}^{1/(n-2)}$, which yields

$$L(L+1) = \frac{1}{\hbar^2}\left(\frac{n}{n-2}\right)^{(n-2)/n}(\mu n C_n)^{2/n}(2\mu E)^{(n-2)/n}. \tag{13}$$

Again, with $L(L+1) \approx L^2$, Eq. (12) reads

$$\sigma_L(E) = \pi\left(\frac{n}{n-2}\right)^{(n-2)/n}(nC_n)^{2/n}(2E)^{-(2/n)}. \tag{14}$$

Expressions for common power laws are listed in Table I, with $n = 3$ appearing in dipole allowed excitation exchange, $n = 4$ in polarization potentials between atoms and ions, and $n = 6$ in van der Waals interactions between ground state atoms.

Combining Eqs. (12) and (11) yields $\sigma_{\rm exc} = \sigma_L \sin^2(\Delta\delta_0)$, which lacks the $\ell = 0$ contribution dominating the Wigner regime ($E \to 0$). Thus, we add the missing s-wave term and obtain the final result:

$$\sigma_{\rm exc}(E) = \left(\frac{\pi}{k^2} + \sigma_L(E)\right)\sin^2\Delta\delta_0(E). \tag{15}$$

This equation explicitly shows how s-wave scattering modulates the Langevin cross section, leading to a signature of the s-wave regime at higher temperatures. It arises from the "phase locking" of $\Delta\eta_\ell$ due to cancellation of the long-range contribution to phase shifts and their insensitivity to ℓ at short range. This led to Eq. (6) and its link to $\Delta\delta_0$ in Eq. (7) using WKB. The applicability of Eq. (15) depends on the details of the potentials and validity of the approximations used. If one potential has ℓ-sensitive turning points, e.g., for $V(r)$ repulsive or attractive but extremely shallow, phase locking cannot occur for high ℓ. The same is true if the long-range cancellation in $\Delta\eta_\ell$ is not adequate, e.g., if the centrifugal barriers for $V_{a/b}$ are different. In cases where $V_{a/b}$ are very different at short range, ΔA_0 might be such that $L(L+1)\Delta A_0$ is significant, requiring Eq. (10) instead of Eq. (11) to be used. Our Eq. (15) also relies on evaluating $A_i(\ell)$ via Eq. (5); if $r_{\rm top} \lesssim R$, the expansion for $A_i(R,\ell)$ will require higher powers of $(\ell+\frac{1}{2})$. Similarly, at high E, even if $R < r_{\rm top}$, $(\ell+\frac{1}{2})^2/r^2$ is significant enough to bring additional ℓ dependence of ΔA and modify Eq. (15). The insensitivity of η_ℓ has been noted in other work, e.g., using multichannel quantum-defect theory to express the scattering K matrix in terms of few parameters [46–49], while the WKB approximation was shown to be useful in related studies [49,50]. We note that phase locking based on WKB was invoked in a study of low spin-flip rate in Ref. [41].

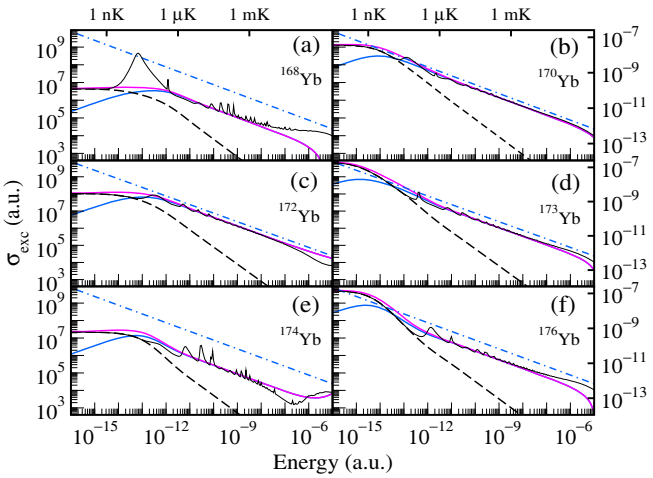

FIG. 2. Resonant charge transfer $\sigma_{\rm exc}$ (right axis: cm^2) for various isotopes of Yb + Yb$^+$ vs scattering energy E (top axis: kelvin). Numerical results (black line) are compared to the standard σ_L (blue dot-dashed line), to Eq. (15) (magenta line), and its components; the s-wave contribution $(\pi/k^2)\sin^2\Delta\delta_0$ (black dashed line) and $\sigma_L \sin^2\Delta\delta_0$ (solid blue line). Isotopes 168 (a), 174 (e), and 176 (f) show significant suppression when compared to σ_L, while 170 (b), 172 (c), and 173 (d), $\sigma_{\rm exc} \approx \frac{1}{2}\sigma_L$ over a wide range of energies.

To illustrate the effect of the s-wave regime at higher energies, we first consider resonant charge transfer between Yb and Yb$^+$ for various isotopes in Fig. 2; as reported in Ref. [51], $\sigma_{\rm exc}$ exhibits a modified Langevin regime strongly affected by the Wigner regime, despite the contribution of many partial waves. Figure 2 compares Eq. (15) to the full numerical results computed using the approach described in Ref. [51], with potentials $V_{g/u}$ corresponding to the $^2\Sigma^+_{g/u}$ states of Yb_2^+ behaving as $-C_4/r^4$ at large separation, with

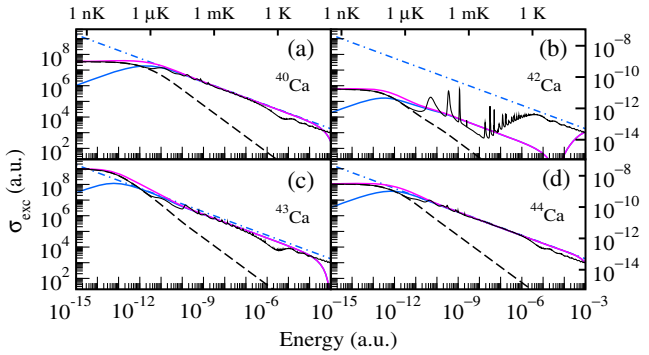

FIG. 3. Same as Fig. 2 for spin flip in $Na + {}^{A}Ca^{+}$, with $A = 40$ (a), 42 (b), 43 (c), and 44 (d). Significant suppression occurs in (b), while σ_{exc} is close to σ_L for the other isotopes. Here, $C_4 = 81.35$ a.u.

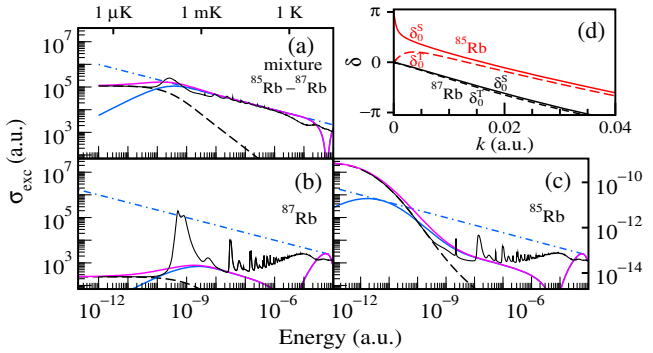

FIG. 4. Same as Fig. 2 for spin-flip collisions in $^{85}Rb + {}^{87}Rb$ mixture (a), pure ^{87}Rb (b), and pure ^{85}Rb (c). Both pure cases exhibit suppression, which reveals shape resonances; indeed, in panel (d) $\delta_0^{S/T}$ show that $\Delta\delta_0$ is small at high E. Here, $C_6 = 4707$ a.u.

$C_4 = 72.5$ a.u. The Langevin cross section σ_L is also shown to emphasize the effect of the s-wave phase shifts. For some isotopes like 170, 172, and 173 shown in Figs. 2(b), 2(c), and 2(d), respectively, σ_{exc} is roughly $\frac{1}{2}\sigma_L$, which is expected as $\langle \sin^2 \Delta\delta_0 \rangle = \frac{1}{2}$ on average if $\Delta\delta_0$ has a random value. However, in other cases like isotopes 168, 174, or 176 in Figs. 2(a), 2(e), and 2(f), respectively, the signature of the s-wave regime is noticeable, with a reduction of 2 orders of magnitude for Figs. 2(a) and 2(e), and 1 for Fig. 2(f). Equation (15) provides the explanation for this unexpected correlation; if the s-wave phase shifts are (accidentally) nearly equal, the phase-locking result of Eq. (7) guarantees the smallness of $\Delta\eta_\ell$ for a wide range of partial waves, yielding a diminished cross section. When the s-wave suppression of σ_{exc} is significant, as in Figs. 2(a) and 2(e), the underlying shape resonances become more apparent as the background cross section diminishes. Naturally, these resonances are absent from our WBK treatment in Eq. (15), which reproduces the general trend of the numerical results over a large range of E. According to Eq. (13), $L^2 < 1$ for $E \lesssim 10^{-13}$ a.u. for this system, at which point the $\ell = 0$ contribution (negligible at higher E) satisfying the Wigner regime kicks in. The *ab initio* potentials $V_{g/u}$ are not accurate enough to predict the s-wave results; however, measurements of the variation of σ_{exc} with isotope at higher energies would provide information to better determine the potentials in a fashion similar to the Feshbach resonances used to adjust the potentials between ground state atoms [1,2].

Atom-ion scattering can also lead to a resonant spin-flip process, such as in $Na + Ca^+$ [52,53] interacting via a singlet (S) $A^1\Sigma^+$ or a triplet (T) $a^3\Sigma^+$ state described by the potentials $V_{S/T}$ and phase shift $\delta_\ell^{S/T}$; σ_{exc} was found to be roughly $\frac{3}{4}\sigma_L$ in Ref. [52]. Recent experiments on $Yb^+ + {}^{87}Rb$ [20], $Yb^+ + {}^{6}Li$ [39], and $^{88}Sr^+ + Rb$ [40,41] have explored spin-flip dynamics. In Fig. 3, we investigate the effect of the s-wave scattering on the spin flip in $Ca^+ + Na$, using $V_{S/T}$ described in Refs. [52,54] (behaving as C_4/r^4 at large r) for four isotopes of Ca, namely, 40, 42, 43, and 44. Again, Eq. (15) agrees with the numerical cross sections over a wide range of energy. Figure 3 shows a variety of behavior; in Figs. 3(a) and 3(d), $\sigma_{exc} \approx \sigma_L$ at higher energies, corresponding to $\Delta\delta_0 = \delta_0^S - \delta_0^T \approx \pi/2$, while Fig. 3(c) depicts a small suppression by a factor of about $\frac{2}{3}$. The case of ^{40}Ca leads to a substantial reduction of about $\frac{1}{200}$, again revealing the underlying shape resonances.

Spin-flip collisions have also been studied between neutral atoms, especially alkali atoms like Li [34] or Na [35], which interact along singlet (S) $X^1\Sigma_g^+$ and triplet (T) $a^3\Sigma_u^+$ states behaving asymptotically as $-C_6/r^6$. We consider ^{87}Rb as the corresponding scattering lengths are nearly equal. Using $V_{S/T}$ described in Ref. [55], we computed σ_{exc} for pure ^{87}Rb, ^{85}Rb, and their mixture. The results are shown in Fig. 4; σ_{exc} for the mixture in Fig. 4(a) follows roughly σ_L away from ultracold temperatures. As expected, for ^{87}Rb in Fig. 4(b) with both singlet and triplet scattering lengths almost equal ($a_S \approx a_T \approx 100$ a.u.), the s-wave suppression is drastic, with shape resonances emerging from the suppressed background. Although not perfect, Eq. (15) tracks the overall reduction of a factor of 10^4 in σ_{exc}. Much more surprising is the result for ^{85}Rb Fig. 4(c) with very different scattering lengths ($a_S \approx 2500$ a.u. and $a_T \approx -390$ a.u.), where one could have expected σ_{exc} to follow σ_L. The s-wave phase shifts in Fig. 4(d) explain the result. The large $a_{S/T}$ imply rapid changes of $\delta_0^{S/T}$ with E (or k) in the Wigner regime. As k grows, $\tan\delta_0^i \approx 2a_i k/(a_i r_i^{\rm eff} k^2 - 2)$ [45] reaches $2/kr_i^{\rm eff}$ if a_i is large, and with effective ranges $r_i^{\rm eff}$ basically the same for ^{85}Rb and ^{87}Rb, the large initial $\Delta\delta_0$ quickly evolves into a value comparable to that of ^{87}Rb.

We consider a final case with r^{-3} long-range potentials. Many examples occur in nature, such as excitation exchange [36] in metastable helium $He(1^1S) + He^*(2^3P)$ [56,57], or in the scattering of metastable atoms like $H(2s) + H(2s)$ [58,59]. Here, we examine $Cs^+ + Cs^*(6p)$, which can lead

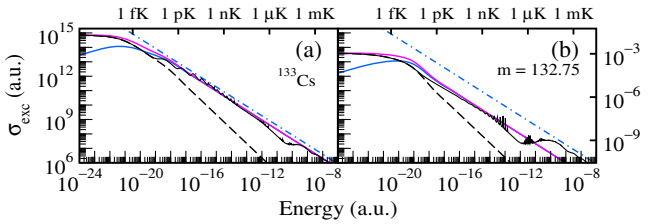

FIG. 5. Same as Fig. 2 for excitation exchange in $^{133}Cs^+ + {}^{133}Cs(6p)$ (a), and for a fictitious mass of 132.75 u (b).

to the exchange of the $6p$ excitation onto Cs^+. Four states are involved if we neglect spin-orbit coupling, two $\Sigma^+_{g/u}$ and two $\Pi_{g/u}$, each correlated to the $Cs_2^+(6p)$ asymptote, and described by potentials $V^{\Sigma}_{g/u}$ and $V^{\Pi}_{g/u}$ and phase shifts $\delta^{g/u}_{\Sigma,\ell}$ and $\delta^{g/u}_{\Pi,\ell}$. Defining $\Delta\delta^{\Sigma}_{\ell} \equiv \delta^{g}_{\Sigma,\ell} - \delta^{u}_{\Sigma,\ell}$ and $\Delta\delta^{\Pi}_{\ell} \equiv \delta^{g}_{\Pi,\ell} - \delta^{u}_{\Pi,\ell}$, we have [36,44]

$$\sigma_{\rm exc} = \frac{\pi}{3k^2}\sum_{\ell=0}^{\infty}(2\ell+1)[\sin^2\Delta\delta^{\Sigma}_{\ell} + 2\sin^2\Delta\delta^{\Pi}_{\ell}]. \quad (16)$$

Since the Σ and Π curves have different C_3 values, L for both sets is different. Using our approximations, $\sigma_{\rm exc}$ becomes

$$\sigma_{\rm exc} = \frac{1}{3}\left[\frac{\pi}{k^2} + \sigma^{\Sigma}_{L}\right]\sin^2\Delta\delta^{\Sigma}_{0} + \frac{2}{3}\left[\frac{\pi}{k^2} + \sigma^{\Pi}_{L}\right]\sin^2\Delta\delta^{\Pi}_{0}, \quad (17)$$

where $\sigma_L^{\Sigma(\Pi)}$ is obtained with the appropriate value of C_3. The results shown in Fig. 5 were obtained with the curves from Jraij *et al.* [60]. The Π curves are repulsive at large separation behaving as $+C_3^{\Pi}/r^3$ ($C_3^{\Pi} = 13.95$ a.u.) with $\delta^{g}_{\Pi,\ell} \approx \delta^{u}_{\Pi,\ell}$ for all ℓ, their cancellation leading to a negligible Π contribution. The two Σ curves are attractive and were matched at large separation to $-C_4/r^4 - C_3/r^3$ with $C_4 = 1082$ a.u., and $C_3^{\Sigma} = 27.9$ a.u. For ^{133}Cs, we find $\sigma_{\rm exc} \approx \frac{1}{2}\sigma_L$, while rescaling its mass to $m_{\rm Cs} = 132.75$ u to simulate a different isotope, $\sigma_{\rm exc}$ is reduced by $\frac{1}{20}$, again exposing resonances as in other cases.

In conclusion, we derived a simple expression for resonant scattering processes that relates the cross section to the Langevin cross section and the s-wave regime. We applied it to various resonant processes like charge transfer, spin flip, and excitation exchange, and for different interaction tails behaving as r^{-n} covering the most common powers. The expression points to the signature of the s-wave regime at higher temperatures and how the $\Delta\delta_0$ phase locking modulates $\sigma_{\rm exc}$. The results presented here also provide a diagnostic tool particularly relevant to a system for which ultracold temperatures are not easily achievable, such as atom-ion hybrid systems for which the nK regime remains a challenge. In fact, by measuring the cross section or rate for a resonant process, e.g., charge transfer or spin flip, at higher temperatures more easily accessible, one can gain information about the s-wave regime. If a sizable suppression is observed as compared to σ_L, this implies that the s-wave phase shifts are close to each other. In addition, the suppression helps reveal shape resonances otherwise submerged which can also help determine the potential curves more accurately. Finally, the expression should be applicable to quasiresonant processes [44], like charge transfer with mixed isotopes [42,43], or in reactions involving different hyperfine asymptotes [33] or isotope substitutions [61,62], as long as the scattering energy is larger than the energy gap between the asymptotes of the relevant potentials.

This work was partially supported by the National Science Foundation Grant No. PHY-1806653 and by the MURI U.S. Army Research Office Grant No. W911NF-14-1-0378.

[1] T. Köhler, K. Góral, and P. S. Julienne, Rev. Mod. Phys. **78**, 1311 (2006).
[2] C. Chin, R. Grimm, P. Julienne, and E. Tiesinga, Rev. Mod. Phys. **82**, 1225 (2010).
[3] A. J. Leggett, Rev. Mod. Phys. **73**, 307 (2001).
[4] S. Giorgini, L. P. Pitaevskii, and S. Stringari, Rev. Mod. Phys. **80**, 1215 (2008).
[5] T. Kraemer, M. Mark, P. Waldburger, J. G. Danzl, C. Chin, B. Engeser, A. D. Lange, K. Pilch, A. Jaakkola, H.-C. Nägerl, and R. Grimm, Nature (London) **440**, 315 (2006).
[6] C. H. Greene, P. Giannakeas, and J. Pérez-Ríos, Rev. Mod. Phys. **89**, 035006 (2017).
[7] I. Bloch, J. Dalibard, and W. Zwerger, Rev. Mod. Phys. **80**, 885 (2008).
[8] I. M. Georgescu, S. Ashhab, and F. Nori, Rev. Mod. Phys. **86**, 153 (2014).
[9] C. Gross and I. Bloch, Science **357**, 995 (2017).
[10] L. D. Carr, D. DeMille, R. V. Krems, and J. Ye, New J. Phys. **11**, 055049 (2009).
[11] O. Dulieu, R. Krems, M. Weidemuller, and S. Willitsch, Phys. Chem. Chem. Phys. **13**, 18703 (2011).
[12] R. Côté and A. Dalgarno, Chem. Phys. Lett. **279**, 50 (1997).
[13] R. Côté and A. Dalgarno, J. Mol. Spectrosc. **195**, 236 (1999).
[14] R. Côté, Adv. At. Mol. Opt. Phys. **65**, 67 (2016).
[15] M. Tomza, K. Jachymski, R. Gerritsma, A. Negretti, T. Calarco, Z. Idziaszek, and P. S. Julienne, arXiv:1708.07832.
[16] A. T. Grier, M. Cetina, F. Oručević, and V. Vuletić, Phys. Rev. Lett. **102**, 223201 (2009).
[17] C. Zipkes, S. Palzer, C. Sias, and M. Köhl, Nature (London) **464**, 388 (2010).
[18] S. Schmid, A. Härter, and J. H. Denschlag, Phys. Rev. Lett. **105**, 133202 (2010).
[19] C. Zipkes, S. Palzer, L. Ratschbacher, C. Sias, and M. Köhl, Phys. Rev. Lett. **105**, 133201 (2010).
[20] L. Ratschbacher, C. Sias, L. Carcagni, J. M. Silver, C. Zipkes, and M. Köhl, Phys. Rev. Lett. **110**, 160402 (2013).
[21] S. Haze, R. Saito, M. Fujinaga, and T. Mukaiyama, Phys. Rev. A **91**, 032709 (2015).

[22] Z. Idziaszek, A. Simoni, T. Calarco, and P. S. Julienne, New J. Phys. **13**, 083005 (2011).
[23] M. Tomza, C. P. Koch, and R. Moszynski, Phys. Rev. A **91**, 042706 (2015).
[24] M. Gacesa and R. Côté, Phys. Rev. A **95**, 062704 (2017).
[25] M. Saffman, T. G. Walker, and K. Mølmer, Rev. Mod. Phys. **82**, 2313 (2010).
[26] M. D. Lukin, M. Fleischhauer, R. Cote, L. M. Duan, D. Jaksch, J. I. Cirac, and P. Zoller, Phys. Rev. Lett. **87**, 037901 (2001).
[27] R. Côté, A. Russell, E. E. Eyler, and P. L. Gould, New J. Phys. **8**, 156 (2006).
[28] B. Yan, S. A. Moses, B. Gadway, J. P. Covey, K. R. Hazzard, A. M. Rey, D. S. Jin, and J. Ye, Nature (London) **501**, 521 (2013).
[29] S. A. Moses, J. P. Covey, M. T. Miecnikowski, D. S. Jin, and J. Ye, Nat. Phys. **13**, 13 (2017).
[30] S. Ospelkaus, K.-K. Ni, G. Quéméner, B. Neyenhuis, D. Wang, M. H. G. de Miranda, J. L. Bohn, J. Ye, and D. S. Jin, Phys. Rev. Lett. **104**, 030402 (2010).
[31] S. Ospelkaus, K. Ni, D. Wang, M. De Miranda, B. Neyenhuis, G. Quéméner, P. Julienne, J. Bohn, D. Jin, and J. Ye, Science **327**, 853 (2010).
[32] F. Scazza, C. Hofrichter, M. Höfer, P. De Groot, I. Bloch, and S. Fölling, Nat. Phys. **10**, 779 (2014).
[33] J. Rui, H. Yang, L. Liu, D.-C. Zhang, Y.-X. Liu, J. Nan, Y.-A. Chen, B. Zhao, and J.-W. Pan, Nat. Phys. **13**, 699 (2017).
[34] R. Côté, A. Dalgarno, and M. J. Jamieson, Phys. Rev. A **50**, 399 (1994).
[35] R. Côté and A. Dalgarno, Phys. Rev. A **50**, 4827 (1994).
[36] M. Bouledroua, A. Dalgarno, and R. Côté, Phys. Rev. A **65**, 012701 (2001).
[37] R. Côté and A. Dalgarno, Phys. Rev. A **62**, 012709 (2000).
[38] R. Côté, Phys. Rev. Lett. **85**, 5316 (2000).
[39] H. Fürst, T. Feldker, N. V. Ewald, J. Joger, M. Tomza, and R. Gerritsma, Phys. Rev. A **98**, 012713 (2018).
[40] T. Sikorsky, Z. Meir, R. Ben-Shlomi, N. Akerman, and R. Ozeri, Nat. Commun. **9**, 920 (2018).
[41] T. Sikorsky, M. Morita, Z. Meir, A. A. Buchachenko, R. Ben-shlomi, N. Akerman, E. Narevicius, T. V. Tscherbul, and R. Ozeri, following Letter, Phys. Rev. Lett. **121**, 173402 (2018).
[42] P. Zhang, E. Bodo, and A. Dalgarno, J. Phys. Chem. A **113**, 15085 (2009).
[43] P. Zhang, A. Dalgarno, R. Côté, and E. Bodo, Phys. Chem. Chem. Phys. **13**, 19026 (2011).
[44] N. Mott and H. Massey, *The Theory of Atomic Collisions*, 3rd ed. (Oxford University Press, London, 1965).
[45] H. Friedrich, *Scattering Theory*, 2nd ed. (Springer, Heidelberg, 2016).
[46] B. Gao, Phys. Rev. Lett. **104**, 213201 (2010).
[47] M. Li and B. Gao, Phys. Rev. A **86**, 012707 (2012).
[48] M. Li, L. You, and B. Gao, Phys. Rev. A **89**, 052704 (2014).
[49] K. Jachymski, M. Krych, P. S. Julienne, and Z. Idziaszek, Phys. Rev. A **90**, 042705 (2014).
[50] K. Sakimoto, Phys. Rev. A **94**, 042701 (2016).
[51] P. Zhang, A. Dalgarno, and R. Côté, Phys. Rev. A **80**, 030703 (2009).
[52] O. P. Makarov, R. Côté, H. Michels, and W. W. Smith, Phys. Rev. A **67**, 042705 (2003).
[53] W. W. Smith, D. S. Goodman, I. Sivarajah, J. E. Wells, S. Banerjee, R. Côté, H. H. Michels, J. A. Mongtomery, and F. A. Narducci, Appl. Phys. B **114**, 75 (2014).
[54] M. Gacesa, J. A. Montgomery, H. H. Michels, and R. Côté, Phys. Rev. A **94**, 013407 (2016).
[55] Z. Li, S. Singh, T. V. Tscherbul, and K. W. Madison, Phys. Rev. A **78**, 022710 (2008).
[56] D. Vrinceanu and H. R. Sadeghpour, New J. Phys. **12**, 065039 (2010).
[57] G. Peach, D. G. Cocks, and I. B. Whittingham, J. Phys. Conf. Ser. **810**, 012003 (2017).
[58] R. C. Forrey, R. Côté, A. Dalgarno, S. Jonsell, A. Saenz, and P. Froelich, Phys. Rev. Lett. **85**, 4245 (2000).
[59] S. Jonsell, A. Saenz, P. Froelich, R. C. Forrey, R. Côté, and A. Dalgarno, Phys. Rev. A **65**, 042501 (2002).
[60] A. Jraij, A. Allouche, M. Korek, and M. Aubert-Frécon, Chem. Phys. **310**, 145 (2005).
[61] J. F. E. Croft, J. Hazra, N. Balakrishnan, and B. K. Kendrick, J. Chem. Phys. **147**, 074302 (2017).
[62] I. Simbotin, S. Ghosal, and R. Côté, Phys. Chem. Chem. Phys. **13**, 19148 (2011).